

chloride and bromo bromide complexes that halide exchange occurs when the compound is heated;²⁷ the racemization of the complex by the same intermolecular (dissociation) process seems likely. However, virtually identical rates and activation energies exhibited by all the complexes studied indicate that bond making or breaking is not rate-determining. This still does not explain why no trans isomer is formed. If the diammine compound racemizes by a dissociation mechanism, anation would be expected. This result is observed in the case of *cis-d*-[Co(en)₂(NH₃)₂]Cl₃. The percent loss of the optical activity is almost equal to that of the *cis* diammine complex when heated (Table I), and a reddish color of the product is observed, indicating that *cis*-[Co(en)₂(NH₃)Cl]Cl₂ is present in the product.

On the other hand, *cis-l*-[Co(en)₂(NH₃)₂](PF₆)₃ is found to racemize, in part, without anation. When heated at 140 °C for 21.8 hr, for example, the complex undergoes 26.4% loss of the optical activity and gives 17.0% racemic *cis* isomer with some reddish byproduct (9.4%), probably *cis*-[Co(en)₂(NH₃)F](PF₆)₂. When heated at 118 °C for 28.2 h, large mass loss is observed despite of no loss of ammonia. This result indicates the formation

of what is probably *cis*-[Co(en)₂(NH₃)₂](PF₆)₂F (loss of PF₆ and lattice water only). However, the reaction is accompanied by 8.4% loss of optical activity (Table I). These results could be interpreted as evidence for a twist process. When the complex is heated at a higher temperature, the dissociation process seems to be more prominent, for a large amount of *cis*-[Co(en)₂(NH₃)F](PF₆)₂ is formed. The difference in the kinetic behavior between the chloride and the PF₆⁻ salts can be explained by different chemical properties between the anions: the anion PF₆⁻ has negligible ability to hydrogen bond with the protons on the nitrogen atoms of the ligand and negligible donor ability in attack on the metal, compared with the case of the anion Cl⁻ (or F⁻). Thus, such properties of anions may be important in determining the solid-state reaction mechanisms of coordination compounds as discussed previously.^{8,9,28} To determine this, we are examining the behavior of nonionic, optically active, octahedral complexes.

Acknowledgment. The work described in this paper was done under the sponsorship of the Petroleum Research Fund, administered by the American Chemical Society, for which the authors express their gratitude.

(27) Schmidt, G. B.; Rössler, K. *Radiochim. Acta* 1966, 5, 123. Rössler, K.; Herr, W. *Angew. Chem., Int. Ed. Engl.* 1967, 6, 993.

(28) Fujiwara, T. *Bull. Chem. Soc. Jpn.* 1983, 56, 122.

Contribution from the Department of Chemistry,
University of Hong Kong, Hong Kong

Stabilization of Transition-Metal Complexes in High Oxidation States by Macrocyclic Tertiary Amines. Electrochemical Generation and Spectroscopic Properties of Novel Dihalogeno and Pseudohalogeno Tetraamine Complexes of Ruthenium(IV)

Chi-Ming Che,* Kwok-Yin Wong, and Chung-Kwong Poon

Received June 18, 1985

1,4,8,12-Tetramethyl-1,4,8,12-tetraazacyclotetradecane (15-TMC) was synthesized by the reaction of 1,4,8,12-tetraazacyclotetradecane with formaldehyde. Reactions of K₂[RuCl₅H₂O] with 15-TMC and 16-TMC (16-TMC = 1,5,9,13-tetramethyl-1,5,9,13-tetraazacyclohexadecane) in ethanol yielded *trans*-[RuLCl₂]Cl (L = 15-TMC and 16-TMC, respectively) in high yields. The syntheses of *trans*-[RuLBr₂]ClO₄ [L = (TMEA)₂ (TMEA = *N,N,N',N'*-tetramethyl-1,2-ethanediamine), 14-TMC (1,4,8,11-tetramethyl-1,4,8,11-tetraazacyclotetradecane), and 15-TMC], *trans*-[Ru(TMEA)₂(NCS)₂]NCS, and *trans*-[Ru(14-TMC)(CH₃CN)₂][ClO₄]₂ are also described. The electrochemistry of *trans*-[RuLX₂]⁺ [L = (TMEA)₂, 14-TMC, 15-TMC, and 16-TMC; X = Cl, Br, and NCO] in acetonitrile were examined. The *E*_f^o values of *trans*-[RuLCl₂]Cl in 2 M HCl have been found to decrease with L in the order 14-TMC > 15-TMC > 16-TMC. Reversible/quasi-reversible Ru(IV)/Ru(III) couples in acetonitrile with *E*_f^o values ranging from 1.05 to 1.27 V vs. the ferrocene couple were observed. Controlled-potential electrolyses of *trans*-[RuLX₂]⁺ at 1.30 V vs. the ferrocene couple generated some novel *trans*-[Ru^{IV}LX₂]²⁺ complexes. The ligand-to-metal charge-transfer transitions in the UV-vis spectra of *trans*-[Ru^{IV}(TMEA)₂X₂]²⁺ have been identified at 410 (X = Cl) and 570 nm (X = Br), which are considerably red-shifted with respect to their Ru(III) counterparts.

Introduction

High-valent ruthenium amine complexes having oxidation states greater than +3 are currently receiving our close attention in view of their potential usefulness as oxidative catalysts. In fact, most of the known mononuclear Ru(IV) and Ru(VI) complexes are largely confined to oxo species although complexes like Ru-(C₅Me₄Et)(CO)Br₃, [Ru(Me₂dtc)₃(PPh₃)]BF₄ (Me₂dtc = dimethyldithiocarbamate), and Ru(bpy)₃⁴⁺ (bpy = 2,2'-bipyridine) have also been reported.¹⁻³ We have recently reported the syn-

thesis of some stable monooxo Ru^{IV}=O³ and dioxo O=Ru^{VI}=O complexes of 14-TMC (1,4,8,11-tetramethyl-1,4,8,11-tetraazacyclotetradecane), 15-TMC (1,4,8,12-tetramethyl-1,4,8,12-tetraazacyclotetradecane), 16-TMC (1,5,9,13-tetramethyl-1,5,9,13-tetraazacyclohexadecane), and TMEA (*N,N,N',N'*-tetramethyl-1,2-ethanediamine)^{5,6} (Figure 1). These tertiary amine ligands, being resistant to oxidation upon coordination to a metal ion, are capable of stabilizing high-valent ruthenium complexes because of their *strong σ-donor properties*. As part of our program to investigate the chemistry of high-valent ruthenium and osmium amine complexes, we describe here the electrochemical generation of some novel Ru(IV) complexes of the type *trans*-[RuLX₂]²⁺ [L = 14-TMC, 15-TMC, 16-TMC, and

(1) Nowell, I. W.; Tabatabaish, K.; White, C. *J. Chem. Soc., Chem. Commun.* 1979, 547.

(2) Given, K. W.; Mattson, B. M.; Pignolet, L. H. *Inorg. Chem.* 1976, 15, 3152.

(3) Gaudiello, J. G.; Sharp, P. R.; Bard, A. J. *J. Am. Chem. Soc.* 1982, 104, 6373.

(4) Che, C.-M.; Wong, K.-Y.; Mak, T. C. W. *J. Chem. Soc., Chem. Commun.* 1985, 546.

(5) Che, C.-M.; Wong, K.-Y.; Poon, C.-K. *Inorg. Chem.* 1985, 24, 1797.

(6) Mak, T. C. W.; Che, C.-M.; Wong, K.-Y. *J. Chem. Soc., Chem. Commun.* 1985, 986.

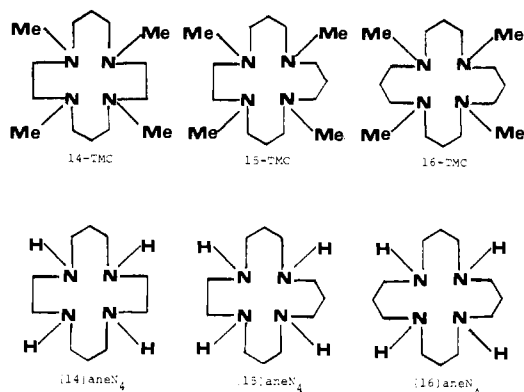


Figure 1. Structures of macrocyclic ligands.

(TMEA)₂; X = Cl, Br, and NCO]. As far as we are aware, this represents the first group of Ru(IV)-saturated amine complexes containing no oxo ligand. These complexes are highly oxidizing with E_7° values as high as +1.30 V vs. the ferrocene couple in CH₃CN. Amine complexes of metal in the +4 oxidation state are rare; the reported ones are those of Pt(IV) and Os(IV).⁷

Experimental Section

Materials. K₂[RuCl₅H₂O] (Johnson Matthey) and 1,4,8,11-tetramethyl-1,4,8,11-tetraazacyclotetradecane (14-TMC) (Strem) were used as supplied. *N,N,N',N'*-Tetramethyl-1,2-ethanediamine (TMEA) was distilled and stored over KOH before used. 1,5,9,13-Tetramethyl-1,5,9,13-tetraazacyclohexadecane (16-TMC),⁸ *trans*-[Ru(LCl₂)ClO₄] [L = (TMEA)₂ and 14-TMC], and *trans*-[Ru(14-TMC)(NCO)₂]ClO₄ were prepared as described previously.⁹ All solvents used were of analytical grade.

1,4,8,12-Tetramethyl-1,4,8,12-tetraazacyclopentadecane (15-TMC) was synthesized by a procedure similar to that used for the preparation of 16-TMC. A mixture of 1,4,8,12-tetraazacyclopentadecane ([15]aneN₄) (Figure 1) (8 g, 0.037 mol), formic acid (40 mL, 98–100%)⁸, formaldehyde (33 mL, 40%), and water (4 mL) was refluxed for 48 h. The reaction mixture was then transferred to a 500-mL beaker containing 50 mL of water, and the contents were cooled to ca. 5 °C in an ice bath. Sodium hydroxide solution (8 M) was added slowly to the solution with stirring until pH > 12. The solution was then extracted with CH₂Cl₂ (3 × 250 mL). The CH₂Cl₂ extracts were combined, dried over anhydrous sodium sulfate, filtered, and evaporated down to an oily residue. This was then distilled under reduced pressure (110 °C, 0.1 mmHg) to give a colorless oil; yield ~80%. ¹H NMR in CDCl₃: δ 1.6 (m, 6 H), 2.2 (m, 12 H), 2.4 (m, 16 H). mass spectral analysis: parent molecular ion at *m/e* 270; IR: no peaks at 3500–3000 cm⁻¹ assignable to ν(N–H). Anal. Calcd for C₁₃H₃₄N₄: C, 66.7; H, 12.6; N, 20.7. Found: C, 66.0; H, 12.4; N, 21.0.

Complexes. *trans*-[Ru(15-TMC)Cl₂]Y (Y = Cl, ClO₄). The complexes were prepared by the controlled dropwise addition method.¹⁰ An ethanolic solution of 15-TMC (0.45 g in 200 mL) was added dropwise to a refluxing ethanolic suspension of K₂[RuCl₅H₂O] (0.5 g in 150 mL) with vigorous stirring. The process took about 5 h to complete, and the mixture was further refluxed for another 12 h. The mixture was then filtered, and the filtrate was evaporated to dryness. A yellow solid was obtained, and this was recrystallized in hot HCl (2 M) to give yellow crystals of *trans*-[Ru(15-TMC)Cl₂]Cl (yield ~39%). *trans*-[Ru(15-TMC)Cl₂]ClO₄ was obtained by the metathesis reaction of the yellow solid with NaClO₄ in 2 M HCl [yield ~65%]. Anal. Calcd for [Ru(15-TMC)Cl₂]ClO₄: C, 33.2; H, 6.3; N, 10.3; Cl, 19.6. Found: C, 33.6; H, 6.5; N, 10.8; Cl, 19.5.

trans-[Ru(16-TMC)Cl₂]Y (Y = Cl, ClO₄). These complexes were similarly prepared as described for *trans*-[Ru(15-TMC)Cl₂]Y except that the 16-TMC ligand was used instead of 15-TMC (yield ~49%). Anal. Calcd for [Ru(16-TMC)Cl₂]ClO₄: C, 34.6; H, 6.5; N, 10.1; Cl, 19.1. Found: C, 34.5; H, 6.6; N, 9.7; Cl, 18.9.

trans-[Ru(LBr₂)]ClO₄ [L = 14-TMC, 15-TMC, (TMEA)₂]. These three complexes were prepared by the same method with similar yields, starting with the appropriate dioxo species. The method is illustrated below for L = 14-TMC. *trans*-[Ru(14-TMC)O₂][ClO₄]₂ (0.3 g) and

ascorbic acid (1 g) were stirred in hot HBr (2 M, 30 mL, 60 °C) for about 20 min. Addition of excess NaClO₄ to the filtered solution immediately deposited the bright orange *trans*-[Ru(14-TMC)Br₂]ClO₄ (yield ~70%). Anal. Calcd for [Ru(14-TMC)Br₂]ClO₄: C, 27.2; H, 5.2; N, 9.1; Cl, 5.8; Br, 26.0. Found: C, 27.6; H, 5.2; N, 9.3; Cl, 5.6; Br, 25.2. Calcd for [Ru(TMEA)₂Br₂]ClO₄: C, 24.3; H, 5.4; N, 9.5; Br, 27.0. Found: C, 24.4; H, 5.9; N, 9.5; Br, 27.4. Calcd for [Ru(15-TMC)Br₂]ClO₄: C, 28.6; H, 5.4; N, 8.9. Found: C, 28.4; H, 5.6; N, 8.9.

trans-[Ru(TMEA)₂(NCS)₂]NCS. *trans*-[Ru(TMEA)₂Cl₂]ClO₄ (0.3 g) and NaNCS (2 g) were stirred in hot water (30 mL) for 1 h. A deep blue solution was obtained. Upon cooling, deep violet-blue *trans*-[Ru(TMEA)₂(NCS)₂]NCS slowly precipitated out. IR (Nujol): ν(C≡N), 2060 cm⁻¹. Anal. Calcd for [Ru(TMEA)₂(NCS)₂]NCS: C, 35.5; H, 6.3; N, 19.3. Found: C, 35.3; H, 6.2; N, 19.2.

trans-[Ru(14-TMC)(CH₃CN)₂]ClO₄₂. *trans*-[Ru(14-TMC)O₂][ClO₄]₂ (0.3 g) and hydrazine hydrate (2 mL) in CH₃CN (30 mL) were stirred for 1 day. Addition of diethyl ether to the resulting solution precipitated *trans*-[Ru(14-TMC)(CH₃CN)₂][ClO₄]₂ as a pale yellow solid. This was recrystallized by slow diffusion of diethyl ether into an acetonitrile solution of the crude product. IR (Nujol): ν(C≡N), 2257 cm⁻¹. Anal. Calcd for [Ru(14-TMC)(CH₃CN)₂][ClO₄]₂: C, 33.9; H, 5.5; N, 13.2; Cl, 11.1. Found: C, 32.8; H, 5.7; N, 13.2; Cl, 11.1.

Physical Measurements. ¹H NMR spectra were run on a JEOL Model (90 MHz) FX90Q spectrometer. UV-vis spectra were measured with a Beckman Acta CIII spectrophotometer.

Cyclic voltammetric measurements were performed by using a PAR universal programmer (Model 175), potentiostat (Model 173), and digital coulometer (Model 179). Formal potentials were taken from the mean values of the cathodic and anodic peak potentials at 25 °C at a scan rate of 100 mV s⁻¹. Cyclic voltammograms were recorded with either a Houston 2000 X-Y recorder at slow scan rates (<500 mV s⁻¹) or a Tektronix model 5441 storage oscilloscope at fast scan rates (>500 mV s⁻¹). Glassy-carbon electrodes were used as the working electrode. All measurements were made against the Ag/AgNO₃ (0.1 M in acetonitrile) electrode. Controlled-potential electrolysis was performed by using a PAR coulometric cell system (Model 9610) equipped with a synchronous stirring motor (Model 377). A platinum-wire gauze or glassy-carbon crucible was used as the working electrode. All reaction solutions were deaerated with argon gas before and during the constant-potential electrolysis. The electrolysis was conducted at a potential that was about 100 mV more positive than the formal potential of the substance to be oxidized.

Acetonitrile (Mallinkrodt Chrom AR) used for electrochemical studies was twice distilled over CaH₂ under argon. Supporting electrolytes were either *n*-tetrabutylammonium fluoborate (0.1 M) or *n*-tetrabutylammonium hexafluorophosphate (0.1 M, electrometric grade, Southwestern Analytical Chemicals Inc.). They were dried in vacuum at 100 °C overnight before being used.

The changing UV-vis spectra during the oxidation of the Ru(III) species were obtained by continually withdrawing samples from a solution undergoing controlled-potential electrolysis and then immediately measuring their spectra. A table of cyclic voltammetric data for the oxidation of *trans*-[Ru(LCl₂)ClO₄] [L = (TMEA)₂ or 14-TMC] (Table T1) and cyclic voltammograms of *trans*-[Ru(TMEA)₂Cl₂]ClO₄ (Figure S1), *trans*-[Ru(15-TMC)Cl₂]ClO₄ (Figure S2), *trans*-[Ru([14]aneN₄)Cl₂]ClO₄ (Figure S3), and *trans*-[Ru(en)₂Cl₂]ClO₄ (Figure S4) are available as supplementary material.

Results and Discussion

The 15-TMC ligand was prepared by the N-methylation reaction of [15]aneN₄, which was like that for 16-TMC except that a longer reaction time was employed. Unlike 14-TMC and 16-TMC, which are crystalline solids, 15-TMC is a colorless oil at room temperature, and this is probably due to its unsymmetrical nature.

Although Taube and co-workers¹¹ were unsuccessful in preparing ruthenium complexes with 15- and 16-membered macrocyclic rings using the synthetic procedure of Chan et al.,^{9,12} we have found the modified controlled dropwise addition method^{8,10} very efficient for the preparation of most ruthenium(III) macrocyclic amine complexes. The yields for *trans*-[Ru(15-TMC)Cl₂]ClO₄ and *trans*-[Ru(16-TMC)Cl₂]ClO₄ were even higher than that for *trans*-[Ru(14-TMC)Cl₂]ClO₄. *trans*-[Ru([16]aneN₄)Cl₂]ClO₄, where [16]aneN₄ represents 1,5,9,13-tetraazacyclo-

(7) Buhr, J. D.; Winkler, J. R.; Taube, H. *Inorg. Chem.* **1980**, *19*, 2416.

(8) Alcock, N. W.; Curzon, E. H.; Moore, P.; Pierpoint, C. *J. Chem. Soc., Dalton Trans.* **1984**, 605.

(9) Che, C.-M.; Kwong, S. S.; Poon, C.-K. *Inorg. Chem.* **1985**, *24*, 1601.

(10) Poon, C.-K.; Che, C.-M. *J. Chem. Soc., Dalton Trans.* **1980**, 756.

(11) Walker, D. D.; Taube, H. *Inorg. Chem.* **1981**, *20*, 2828.

(12) Chan, P. K.; Isabirye, D. A.; Poon, C.-K. *Inorg. Chem.* **1975**, *14*, 2579.

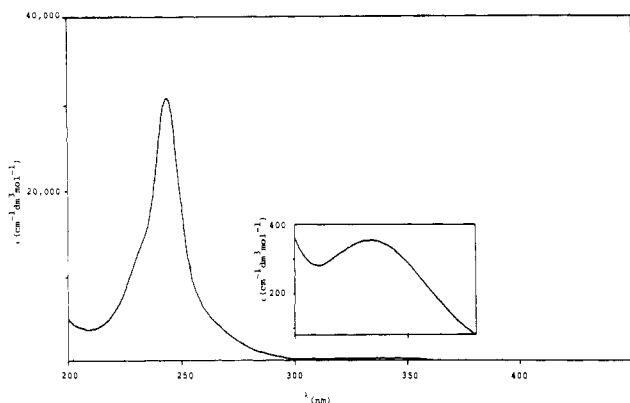


Figure 2. Electronic absorption spectrum of $trans\text{-[Ru}^{\text{II}}(14\text{-TMC)}\text{-(CH}_3\text{CN)}_2\text{]ClO}_4\text{)}_2$ in acetonitrile.

Table I. Summary of Electronic Absorption Spectral Data of Dichlorotetraammineruthenium(III) Complexes

complex	solvent	$\lambda_{\text{max}}/\text{nm}^a$
$trans\text{-[Ru(14-TMC)Cl}_2\text{]ClO}_4^b$	0.1 M HCl	370 (2340); 315 (805)
$trans\text{-[Ru(15-TMC)Cl}_2\text{]Cl}$	0.1 M HCl	372 (2140); ~325 (sh) (760)
$trans\text{-[Ru(16-TMC)Cl}_2\text{]Cl}$	0.1 M HCl	369 (2630); ~320 (sh) (830)
$trans\text{-[Ru([14]aneN}_4\text{)Cl}_2\text{]Cl}^c$	H ₂ O	358 (2560); 315 (1230)
$trans\text{-[Ru([15]aneN}_4\text{)Cl}_2\text{]Cl}^c$	H ₂ O	359 (2410); 317 (1350)
$trans\text{-[Ru([16]aneN}_4\text{)Cl}_2\text{]Cl}^c$	H ₂ O	360 (2320); 318 (1320)
$trans\text{-[Ru(TMEA)}_2\text{Br}_2\text{]ClO}_4$	CH ₃ CN	467 (6390); 370 (585)
$trans\text{-[Ru(14-TMC)Br}_2\text{]ClO}_4$	CH ₃ CN	471 (3990); ~370 (468)
$trans\text{-[Ru(15-TMC)Br}_2\text{]ClO}_4$	CH ₃ CN	471 (4280); ~370 (480)
$trans\text{-[Ru(TMEA)}_2\text{(NCS)}_2\text{]NCS}$	CH ₃ CN	630 (20 140)

^a $\epsilon_{\text{max}}/(\text{cm}^{-1} \text{ dm}^3 \text{ mol}^{-1})$ in parentheses; sh = shoulder. ^b Reference 9. ^c Reference 11.

hexadecane, can also be obtained in high yield by the same method. In general, dibromo(tetraamine)ruthenium(III) complexes of the type $trans\text{-[RuLBr}_2\text{]}^+$ can be most conveniently prepared by the ascorbic acid reduction of the corresponding $trans\text{-[RuLO}_2\text{]}^{2+}$ complex in the presence of Br⁻. Reduction of $trans\text{-[Ru(14-TMC)O}_2\text{]}^{2+}$ by hydrazine hydrate in acetonitrile, however, yielded a Ru(II) species, $trans\text{-[Ru(14-TMC)(CH}_3\text{CN)}_2\text{]ClO}_4$, which has been found to be diamagnetic. The spectrum of $trans\text{-[Ru(14-TMC)(CH}_3\text{CN)}_2\text{]}^{2+}$ (Figure 2) is also similar to that of $trans\text{-[Ru(NH}_3\text{)}_4\text{(CH}_3\text{CN)}_2\text{]}^{2+}$.^{10,13} The 345- and 244-nm bands in the former are, accordingly, assigned as the d-d and $d_{\pi}(\text{Ru}) \rightarrow \pi^*(\text{CH}_3\text{CN})$ transitions, respectively.

A summary of electronic absorption spectral data of the newly prepared and related dichlororuthenium(III) complexes is given in Table I. It is apparent that ring size has virtually no effect on the lowest $p_{\pi}(\text{Cl}) \rightarrow d_{\pi}(\text{Ru})$ transition. The similarities between the UV-vis spectra of the TMC complexes and those of the known $trans$ -dichloro(tetraamine)ruthenium(III) complexes^{11,14} suggest a $trans$ configuration for the new complexes. Moreover, $trans\text{-[Ru(15-TMC)O}_2\text{]ClO}_4$ and $trans\text{-[Ru(16-TMC)O}_2\text{]ClO}_4$, prepared from the corresponding $[\text{RuLCl}_2]\text{ClO}_4$ (L = 15- or 16-TMC) species, have been characterized by X-ray crystallography.⁶ Hence a $trans$ configuration for $trans\text{-[Ru(15-TMC)Cl}_2\text{]}^+$ and $trans\text{-[Ru(16-TMC)Cl}_2\text{]}$ is assigned.

With the exceptions of $trans\text{-[RuLBr}_2\text{]}^+$ and $trans\text{-[Ru(14-TMC)Cl}_2\text{]}^+$ complexes, most ruthenium(III) tertiary amine complexes undergo one-electron reversible/quasi-reversible re-

Table II. Formal Reduction Potentials of $trans\text{-[RuLX}_2\text{]}^+$ in Acetonitrile^a

complex ^b	$E_f^\circ/\text{V}^{c,d}$	
	Ru(II/III)	Ru(III/IV)
$trans\text{-[Ru(14-TMC)Cl}_2\text{]}^+$	-0.56	+1.21
$trans\text{-[Ru(15-TMC)Cl}_2\text{]}^+$	-0.57	+1.21
$trans\text{-[Ru(16-TMC)Cl}_2\text{]}^+$	-0.54	+1.22
$trans\text{-[Ru(TMEA)}_2\text{Cl}_2\text{]}^+$	-0.54	+1.33
$trans\text{-[Ru(14-TMC)Br}_2\text{]}^+$	-0.36 ^e	+1.23
$trans\text{-[Ru(15-TMC)Br}_2\text{]}^+$	-0.39 ^e	+1.18
$trans\text{-[Ru(TMEA)}_2\text{Br}_2\text{]}^+$	-0.41 ^e	+1.22
$trans\text{-[Ru(14-TMC)(NCO)}_2\text{]}^+$	-0.53	+1.13
$trans\text{-[Ru(14-TMC)(NCS)}_2\text{]}^+$	-0.15	
$trans\text{-[Ru(TMEA)}_2\text{(NCS)}_2\text{]}^+$	-0.08	
$trans\text{-[Ru(en)}_2\text{Cl}_2\text{]}^+$	-1.13	+1.31 ^e
$trans\text{-[Ru(14aneN}_4\text{)Cl}_2\text{]}^+$	-0.94	+1.34 ^e
$trans\text{-[Ru(tet a)Cl}_2\text{]}^+$	-0.71	+1.30 ^e
$trans\text{-[Ru(2,3,2-tet)Cl}_2\text{]}^+$	-0.96	+1.18 ^e
$trans\text{-[Ru(en)}_2\text{Br}_2\text{]}^+$	-0.88	+1.18 ^e
$trans\text{-[Ru(tet a)Br}_2\text{]}^+$	-0.57	+1.30 ^e

^a Supporting electrolyte: 0.1 M *n*-tetrabutylammonium fluoborate, except as indicated. ^b Abbreviations: tet a = *C-meso*-5,5,7,12,12,14-hexamethyl-1,4,8,11-tetraazacyclotetradecane; 2,3,2-tet = 3,7-diazanone-1,4-diamine. ^c Vs. Ag/AgNO₃, 0.1 M in CH₃CN. The formal potential $E_f = (E_{pc} + E_{pa})/2$ at 25 °C for reversible couples. For irreversible waves, the peak potential is measured at a scan rate of 100 mV s⁻¹ at 25 °C. The ferrocene couple was found to be +0.060 vs. the Ag/AgNO₃ (0.1 M in CH₃CN) reference electrode. ^d Supporting electrolyte: 0.1 M *n*-tetrabutylammonium perchlorate. ^e Irreversible waves.

Table III. Formal Reduction Potentials of $trans\text{-[RuLCl}_2\text{]Cl}$ in Aqueous Solution

complex	supporting electrolyte	E_f°/V^d
$trans\text{-[Ru(14-TMC)Cl}_2\text{]Cl}^a$	2 M HCl	+0.140
$trans\text{-[Ru(15-TMC)Cl}_2\text{]Cl}$	2 M HCl	+0.036
$trans\text{-[Ru(16-TMC)Cl}_2\text{]Cl}$	2 M HCl	+0.001
$trans\text{-[Ru([14]aneN}_4\text{)Cl}_2\text{]Cl}^b$	0.1 M HCl	-0.150
$trans\text{-[Ru([15]aneN}_4\text{)Cl}_2\text{]Cl}^b$	0.1 M HCl	-0.125
$trans\text{-[Ru([16]aneN}_4\text{)Cl}_2\text{]Cl}^b$	0.1 M HCl	-0.095
$trans\text{-[Ru(TMEA)}_2\text{Cl}_2\text{]Cl}^a$	2 M HCl	+0.14
$trans\text{-[Ru(en)}_2\text{Cl}_2\text{]Cl}^c$	H ₂ O	-0.188

^a Reference 7. ^b Reference 11. ^c Poon, C.-K.; Che, C.-M.; Kan, Y. P. *J. Chem. Soc., Dalton Trans.* 1980, 128. ^d Vs. NHE.

duction in acetonitrile. Their formal reduction potentials, E_f° , and those of analogous secondary and primary amine complexes in acetonitrile and water are collected in Tables II and III. It is interesting to note that the E_f° values for the TMC complexes in 2 M HCl decrease with increasing ring size (i.e., 16-TMC < 15-TMC < 14-TMC) whereas those for the nonmethylated parent complexes show an opposite behavior [i.e., [16]aneN₄ > [15]aneN₄ > [14]aneN₄ (1,4,8,11-tetraazacyclotetradecane) (Figure 1)]. It is also clear from Table II that the E_f° values of $trans\text{-[Ru(14-TMC)Cl}_2\text{]}^+$ and $trans\text{-[Ru(TMEA)}_2\text{Cl}_2\text{]}^+$ in both water and acetonitrile are ~400 mV higher than those of $trans\text{-[Ru([14]aneN}_4\text{)Cl}_2\text{]}^+$ and $trans\text{-[Ru(en)}_2\text{Cl}_2\text{]}^+$ (en = 1,2-diaminoethane) respectively. The reason underlying this is not clear. It could be argued that the absence of any dipolar interaction between the N-H group and the solvent in tertiary amine complexes would tend to destabilize the Ru(III) more than the Ru(II) state.

The cyclic voltammograms of some dichloro complexes are shown in Figure 3. The irreversible nature of the reduction of $trans\text{-[Ru(14-TMC)Cl}_2\text{]}^+$ (Figure 3a) might arise from the rapid solvolysis of $trans\text{-[Ru(14-TMC)Cl}_2\text{]}^+$. Since the E_f° value for the $trans\text{-[Ru(14-TMC)(CH}_3\text{CN)}_2\text{]}^{3+/2+}$ couple is 0.76 V vs. ferrocene, it is reasonable to assume that the observed couple at 0.15 V vs. ferrocene in the first reversed scan (reoxidation) in the cyclic voltammogram of $trans\text{-[Ru(14-TMC)Cl}_2\text{]}^+$ can be taken to represent the $trans\text{-[Ru(14-TMC)(CH}_3\text{CN)Cl]}^{2+/+}$ couple. The electrochemical behavior of other dichloro tertiary amine complexes is quite different. The $trans\text{-[Ru(TMEA)}_2\text{Cl}_2\text{]}^{+/0}$ (Figure S1) and $trans\text{-[Ru(16-TMC)Cl}_2\text{]}^{+/0}$ (Figure 3b) couples

(13) Clarke, R. E.; Ford, P. C. *Inorg. Chem.* 1970, 9, 227.

(14) Poon, C.-K.; Lau, T. C.; Che, C.-M. *Inorg. Chem.* 1983, 22, 3893.

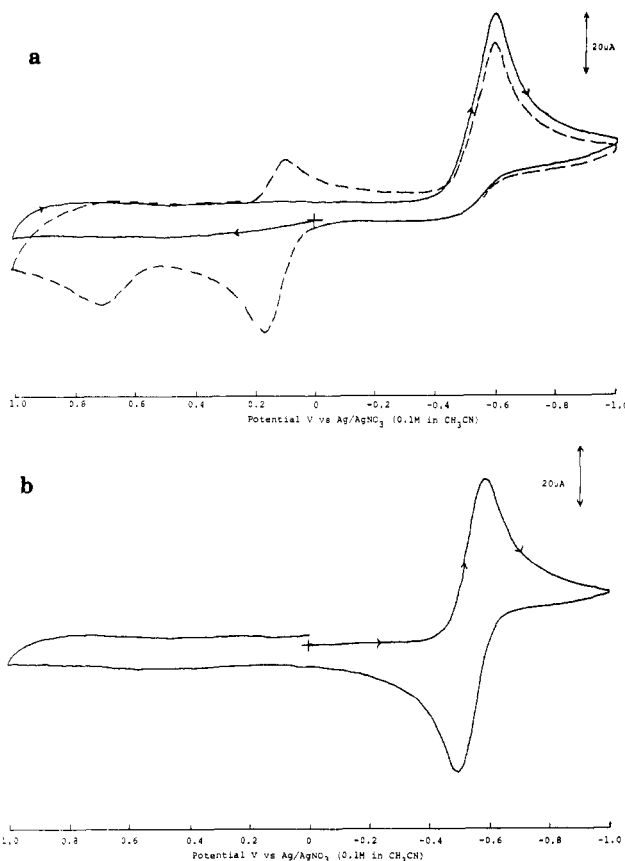


Figure 3. Cyclic voltammograms showing the reduction of (a) $\text{trans-[Ru(14-TMC)Cl}_2\text{]ClO}_4$ and (b) $\text{trans-[Ru(16-TMC)Cl}_2\text{]ClO}_4$ in acetonitrile (0.1 M *n*-tetrabutylammonium fluoroborate, 100 mV s^{-1} , and glassy-carbon electrode).

are nearly reversible with $i_{pa}/i_{pc} = 1$ (scan rate 100 mV s^{-1}). For the $\text{trans-[Ru(15-TMC)Cl}_2\text{]}^{+/0}$ couple, the i_{pc}/i_{pa} ratio is about 0.72 (scan rate 100 mV s^{-1}). This indicates that the extent of solvolysis of $\text{trans-[RuLCl}_2\text{]}^0$ decreases with $\text{L} = 14\text{-TMC} > 15\text{-TMC} > 16\text{-TMC} \sim (\text{TMEA})_2$. The result is understandable in view of the release of steric constraint between the N-CH_3 and the axial Ru-Cl groups with increasing size of macrocycles. This kind of steric constraint is naturally smallest in $(\text{TMEA})_2$ among the above series of tertiary amine complexes.

An outstanding feature of the electrochemistry of the tertiary amine complexes in acetonitrile is the presence of reversible/quasi-reversible Ru(IV)/Ru(III) couples (Table II) with E_f° values at about 1.1 V vs. the ferrocene/ferrocenium couple. In cases of primary and secondary amine complexes of ruthenium(III), such as $\text{trans-[Ru([14]aneN}_4\text{)Cl}_2\text{]}^+$ and $\text{trans-[Ru(en)}_2\text{Cl}_2\text{]}^+$, the electrochemical oxidation of Ru(III) to Ru(IV) (Figures S3 and S4) is irreversible, and this is understandable as the strongly oxidizing Ru(IV) center would easily oxidize the coordinated amine (-NH-CHR) group to an imine (-N=CR) group.¹⁵ For $\text{trans-[Ru(14-TMC)Cl}_2\text{]}^+$ (Figure 4) and $\text{trans-[Ru(TMEA)}_2\text{Cl}_2\text{]}^+$ (Figure S1) complexes, at scan rates faster than 10 mV s^{-1} , the Ru(IV)/Ru(III) couple appears to be quasi-reversible. As the scan rate increases, the peak-to-peak separation (ΔE_p) widens while the current function ($i_{pa}/v^{1/2}$) and the current ratio ($i_{pc}/i_{pa} = 1$) remain constant (Table T1). Similar results for other $\text{trans-[RuLX}_2\text{]}^+$ species have also been found. However, at very slow scan rates, the current function $i_{pa}/v^{1/2}$ is larger than the constant value found at fast scan rates, and i_{pc}/i_{pa} is smaller than unity. Moreover, controlled-potential coulometric oxidation of ruthenium(III) complexes showed that the oxidative current did not decay to a background level but rather remained at a constant value as oxidation proceeded. For $\text{trans-[Ru(TMEA)}_2\text{Cl}_2\text{]}^+$ and $\text{trans-[Ru(16-TMC)Cl}_2\text{]}^+$, the cyclic volt-

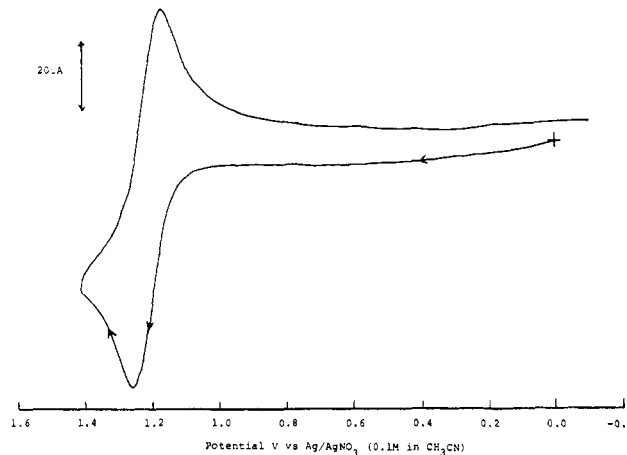


Figure 4. Cyclic voltammograms showing the oxidation of $\text{trans-[Ru(14-TMC)Cl}_2\text{]ClO}_4$ in acetonitrile (0.1 M *n*-tetrabutylammonium fluoroborate, 100 mV s^{-1} , and glassy carbon electrode).

ammograms of the solution before and after 1 equiv of coulombs needed for complete oxidation for a one-electron process have passed are the same. Qualitatively, these results are in accordance with the picture that the electrochemically generated Ru(IV) complex reacts with nonelectroactive species (possibly acetonitrile) to regenerate the starting material. Similar findings on $\text{Ru}^{\text{IV}}(\text{bpy})_3^{4+3}$ have also been observed. The electrochemical oxidation of $\text{trans-[RuLX}_2\text{]}^+$ is essentially metal-centered since in the analogous $\text{trans-[Os(14-TMC)X}_2\text{]}^+$ complexes, the E_f° value of the Os(IV)/Os(III) couple is at 0.6–0.7 V vs. the ferrocene/ferrocenium couple.¹⁶ As in case of the osmium(IV) amine complexes,⁷ the E_f° values for the $\text{trans-[RuLX}_2\text{]}^{2+/+}$ couple (Table II) are quite insensitive to the nature of the axial ligand X. It is also interesting to note that the macrocyclic ring size does not affect the E_f° values for both the Ru(III)/Ru(II) and Ru(IV)/Ru(III) couples.

$\text{trans-[Ru}^{\text{IV}}(\text{TMEA})_2\text{X}_2\text{]}^{2+}$ ($\text{X} = \text{Cl}$ and Br) complexes have also been characterized spectroscopically. The UV-vis spectral changes during the electrochemical oxidations of $\text{trans-[Ru(TMEA)}_2\text{Cl}_2\text{]}^+$ and $\text{trans-[Ru(TMEA)}_2\text{Br}_2\text{]}^+$ in acetonitrile are shown in Figure 5. In both cases, isosbestic points were maintained throughout the oxidations. For $\text{trans-[Ru(TMEA)}_2\text{Cl}_2\text{]}^+$, the 367-nm band ($p_x(\text{Cl}) \rightarrow d_x^*[\text{Ru(III)}]$ transition) gradually disappeared and a new band at 410 nm developed. The 410-nm species is not a $\text{Ru}^{\text{IV}}=\text{O}$ complex as the analogous $\text{trans-[Ru}^{\text{IV}}(\text{14-TMC})(\text{O})(\text{CH}_3\text{CN})]^{2+}$ and $\text{trans-[Ru}^{\text{IV}}(\text{14-TMC})(\text{O})(\text{Cl})]^{2+}$ species do not absorb strongly at $\lambda > 350$ nm.^{16,17} As in case of osmium amine complexes⁷ where ligand-to-metal charge-transfer transitions are red-shifted from Os(III) to Os(IV) , the 410-nm band could be assigned as the $p_x(\text{Cl}) \rightarrow d_x^*[\text{Ru(IV)}]$ transition of $\text{trans-[Ru}^{\text{IV}}(\text{TMEA})_2\text{Cl}_2\text{]}^{2+}$. The assignment was supported by the observation that the band was red-shifted to 570 nm in $\text{trans-[Ru}^{\text{IV}}(\text{TMEA})_2\text{Br}_2\text{]}^{2+}$. Addition of hydroquinone to the electrogenerated solution of $\text{trans-[Ru}^{\text{IV}}(\text{TMEA})_2\text{Cl}_2\text{]}^{2+}$ / $\text{trans-[Ru}^{\text{IV}}(\text{TMEA})_2\text{Br}_2\text{]}^{2+}$ led to immediate disappearance of the 410-nm/570-nm species with over 95% recovery of the original $\text{trans-[Ru(TMEA)}_2\text{Cl}_2\text{]}^+$ / $\text{trans-[Ru(TMEA)}_2\text{Br}_2\text{]}^+$ complex, thus indicating that the 410-nm/570-nm species is not the product of subsequent irreversible chemical reactions of $\text{trans-[Ru}^{\text{IV}}(\text{TMEA})_2\text{Cl}_2\text{]}^{2+}$ / $\text{trans-[Ru}^{\text{IV}}(\text{TMEA})_2\text{Br}_2\text{]}^{2+}$. Similar results have also been observed for $\text{trans-[Ru(16-TMC)Cl}_2\text{]}^+$ ($\text{trans-[Ru}^{\text{IV}}(\text{16-TMC)Cl}_2\text{]}^{2+}$, $\lambda_{\text{max}} \sim 410$ nm). However, for the 14-TMC and 15-TMC complexes, the UV-vis spectral changes during the constant-potential coulometric oxidations are quite complex with ill-defined isosbestic points. Presumably, the Ru(IV) complexes of 14-TMC and 15-TMC are less stable than those of TMEA and 16-TMC species.

(16) Che, C.-M.; Cheng, W. K.; Wong, K.-Y., unpublished results.

(17) Che, C.-M.; Wong, K.-Y.; Mak, T. C. W. *J. Chem. Soc., Chem. Commun.* **1985**, 988.

(15) Mahoney, D. F.; Beattie, J. K. *Inorg. Chem.* **1973**, *12*, 2561.

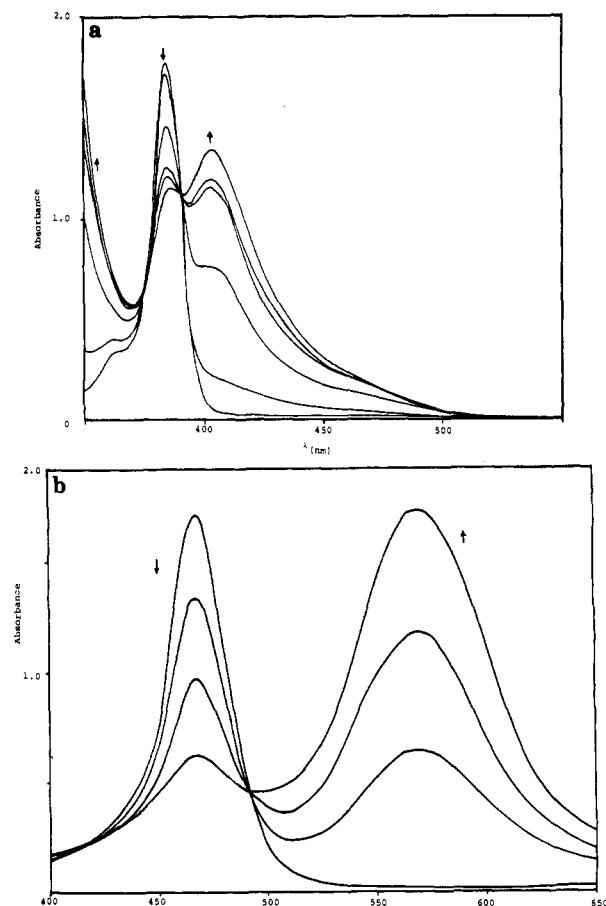


Figure 5. Spectral changes during the electrochemical oxidation of (a) $\text{trans-[Ru(TMEA)}_2\text{Cl}_2\text{]ClO}_4$ (0.58 mM) and (b) $\text{trans-[Ru(TMEA)}_2\text{Br}_2\text{]ClO}_4$ (0.31 mM) in 0.1 M ($n\text{-Bu}_4\text{N}$)PF₆ acetonitrile solution (potential held at +1.30 V vs. Ag/Ag⁺ reference electrode; working electrode, platinum gauze).

Table IV. Voltammetric Data for the Oxidation of $\text{trans-[Ru(TMEA)}_2\text{Cl}_2\text{]ClO}_4$ with or without the Addition of 2-Propanol

scan rate/ mV s ⁻¹	without 2-propanol		with 2-propanol (5% v/v)	
	$i_{pa}/\mu\text{A}$	i_{pc}/i_{pa}	$i_{pa}/\mu\text{A}$	i_{pc}/i_{pa}
5	22.0	0.80	34.5	^a
10	29.0	0.95	37.0	0.67
20	41.0	0.98	48.0	0.76
50	65.5	0.99	70.0	0.89
100	92.0	0.97	96.0	0.92
200	130.0	0.99	130.0	0.99

^aNo cathodic peaks.

The results here clearly demonstrate for the first time the electrochemical generation of some highly oxidizing mononuclear Ru(IV) complexes containing no oxo ligand. The potential usefulness of tertiary amine ligands in the stabilization of highly oxidizing metal complexes is also implied. In order to test the applicability of $\text{trans-[Ru}^{\text{IV}}\text{LX}_2\text{]}^{2+}$ as useful electrochemical oxidative catalysts, the electrochemistry of $\text{trans-[Ru(TMEA)}_2\text{Cl}_2\text{]}^+$ in the presence of added 2-propanol was studied (Table IV). At scan rates less than 50 mV s⁻¹, the anodic peak currents are larger

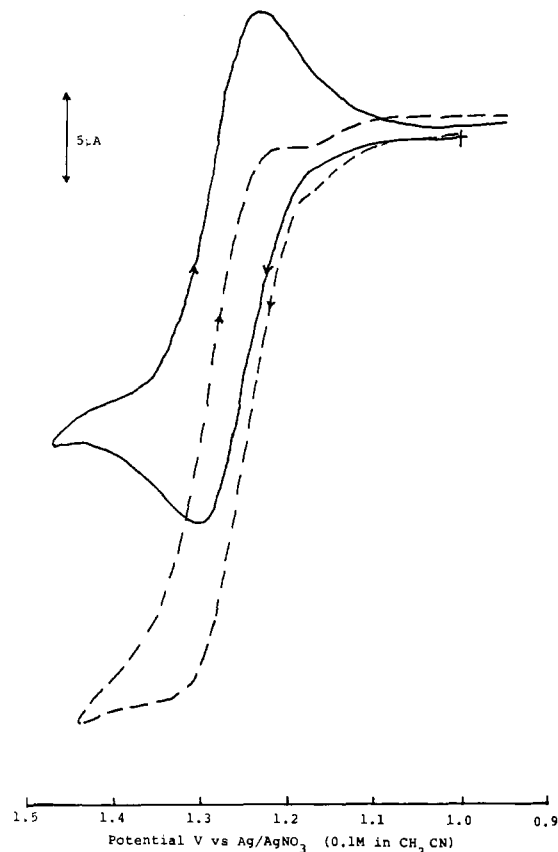


Figure 6. Cyclic voltammograms for the oxidation of $\text{trans-[Ru(TMEA)}_2\text{Cl}_2\text{]ClO}_4$ (3 mM) in acetonitrile in the absence of 2-propanol (—) and in the presence of 2-propanol (0.65 M) (---). Scan rate: 5 mV s⁻¹.

than those in the absence of 2-propanol. The current ratio (i_{pc}/i_{pa}) decreases with decreasing scan rates. A polarographically shaped catalytic wave (Figure 6) was observed at 2–5 mV s⁻¹. This showed that 2-propanol could be catalytically oxidized by $\text{trans-[Ru}^{\text{IV}}\text{(TMEA)}_2\text{Cl}_2\text{]}^{2+}$ at the electrode.

It should be pointed out, however, that despite the high E_f° values for these Ru(IV)/Ru(III) couples, the rates of these catalytic reactions were not necessarily fast. As an illustration, for $\text{trans-[Ru(TMEA)}_2\text{Cl}_2\text{]}^{2+}$, no catalytic current was observed at scan rates greater than 100 mV s⁻¹. It is premature to attempt to discuss the mechanism of this catalytic oxidative reaction although a free-radical pathway is likely to take place. Much work employing this class of Ru(IV) complexes as active electrooxidative catalysts is in progress.

Acknowledgment. We thank the Committee on Research and Conference Grants of the University of Hong Kong for financial support. K.-Y.W. further acknowledges the award of a Higher Degree Studentship from the University. Helpful discussions with Dr. K. W. Fung are also acknowledged.

Supplementary Material Available: Cyclic voltammograms of $\text{trans-[Ru(TMEA)}_2\text{Cl}_2\text{]ClO}_4$ (Figure S1), $\text{trans-[Ru(15-TMC)Cl}_2\text{]ClO}_4$ (Figure S2), $\text{trans-[Ru([14]aneN}_4\text{)Cl}_2\text{]ClO}_4$ (Figure S3), and $\text{trans-[Ru(en)}_2\text{Cl}_2\text{]ClO}_4$ (Figure S4) in acetonitrile and a table of cyclic voltammetric data for the oxidation of $\text{trans-[RuLCl}_2\text{]ClO}_4$ [L = 14-TMC or (TMEA)₂] (Table T1) (4 pages). Ordering information is given on any current masthead page.